Metagenomic insights into the inhibitory mechanisms of Cu on fermentative hydrogen production

Jinman Cao [a,b], Guilan Duan [a,c], Aijun Lin [b], Yaoyu Zhou [d], Siming You [e], Jonathan W.C. Wong [f], Guang Yang [a,*]

[a] State Key Lab of Urban and Regional Ecology, Research Center for Eco-Environmental Sciences, Chinese Academy of Sciences, Beijing 100085, China

[b] College of Chemical Engineering, Beijing University of Chemical Technology, Beijing 100029, PR China

[c] University of Chinese Academy of Sciences, Beijing 100049, China

[d] College of Resources and Environment, Hunan Agricultural University, Changsha 410128, China

[e] James Watt School of Engineering, University of Glasgow, Glasgow, G128QQ, UK

[f] Sino-Forest Applied Research Centre for Pearl River Delta Environment, Department of Biology, Hong Kong Baptist University, China

* Corresponding author

Dr. Guang Yang

E-mail: guangyang@rcees.ac.cn

[*] Corresponding author, E-mail: guangyang@rcees.ac.cn

Abstract:

Cu is widely present in the feedstocks of dark fermentation, which can inhibit H_2 production efficiency of the process. However, current understanding on the inhibitory mechanisms of Cu, especially the microbiological mechanism, is still lacking. This study investigated the inhibitory mechanisms of Cu^{2+} on fermentative hydrogen production by metagenomics sequencing. Results showed that the exposure to Cu^{2+} reduced the abundances of high-yielding hydrogen-producing genera (e.g. *Clostridium sensu stricto*), and remarkably down-regulated the genes involved in substrate membrane transport (e.g., *gtsA*, *gtsB* and *gtsC*), glycolysis (e.g. *PK*, *ppgK* and *pgi-pmi*), and hydrogen formation (e.g. *pflA*, *fdoG*, *por* and *E1.12.7.2*), leading to significant inhibition on the process performances. The H_2 yield was reduced from 1.49 mol H_2/mol-glucose to 0.59 and 0.05 mol H_2/mol-glucose upon exposure to 500 and 1000 mg/L of Cu^{2+}, respectively. High concentrations of Cu^{2+} also reduced the rate of H_2 production and prolonged the H_2-producing lag phase.

Keywords: Cu; Fermentative hydrogen production; Inhibition; Microbial community structure; Metagenomic analysis

1. Introduction

Hydrogen energy is a promising substitute to fossil fuels, because of its advantages of pollution-free combustion applications and high energy density (Fan et al., 2022). At present, the main hydrogen production technologies are steam reforming and gasification using fossil fuels (Dahiya et al., 2021). However, these traditional H_2-producing methods are environmentally unfriendly and cost-intensive.

Therefore, it is desired to develop alternative technologies to produce hydrogen in an environmentally friendly way.

Biological dark fermentation has been regarded as one of the most sustainable technologies to produce hydrogen, because of its low energy requirement, environment protection, and easy operation conditions (Cheng et al., 2022). What makes dark fermentation more attractive is its capability to utilize multiple organic wastes (e.g. livestock manure, agroforestry wastes, food wastes, sewage sludge and wastewater) to produce hydrogen (Arun et al., 2022; Khoufi et al., 2015; Sillero et al., 2022). Despite the strengths of dark fermentation, a low hydrogen yield is the primary limitation of this process, which restricts its scale-up and wide application (Ren et al., 2022). It has been reported that inhibitors presenting in the reactor, such as toxic organics and heavy metals, are some of the major factors limiting hydrogen yields for dark fermentation (Bundhoo and Mohee, 2016). Among various inhibitory substances, heavy metals have drawn particular attentions, owing to its high toxicity and wide presence in hydrogen fermentation reactors (Chen et al., 2021; Elbeshbishy et al., 2017). Numerous studies have been conducted to examine the inhibitory effect of heavy metals on the efficiency of dark hydrogen fermentation (Sharma and Melkania, 2018; Lin and Shei, 2008; Chen et al., 2021; Matyakubov et al., 2022).

Copper (Cu), a typical heavy metal, has been frequently detected in the feedstocks of dark fermentation, such as wastewater (Al-Saydeh et al., 2017), municipal solid waste (Sharma and Melkania, 2018), livestock manure (Liu et al., 2020), and sewage sludge (Chu and He, 2021). The concentrations of Cu can be up to 1751 mg/kg total solids (TS), 422 mg/kg TS, 259.3 mg/L, and 1726 mg/kg dry weight

47 in sewage sludge (Chu and He, 2021), municipal solid waste (Moreno et al., 2013),
48 wastewater (Urrutia et al., 2019), and livestock manure (Guan et al., 2011),
49 respectively. In general, trace concentrations of Cu is necessary for bacterial growth
50 and activating some enzymes and co-enzymes (Sivagurunathan et al., 2015), while a
51 relatively high concentration of Cu is inhibitory and toxic to microorganisms (Chen et
52 al., 2021), because it can disturb the uptake of nutrients, alter bacterial protein
53 synthesis, cause DNA damage, and destroy the integrity of cell membrane. Some
54 studies found that Cu could inhibit the hydrogen production during dark fermentation
55 (Li and Fang, 2007; Sharma and Melkania, 2018; Lin and Shei, 2008), and the
56 inhibition degree of Cu was greater compared to Cr, Zn, Cd, Ni, and Pb (Li and Fang,
57 2007). Nevertheless, most previous studies concentrated on the inhibition effect of Cu
58 on dark fermentation performances, including H_2 production, substrate utilization, and
59 liquid metabolites generation (Li and Fang, 2007; Sharma and Melkania, 2018; Chen
60 et al., 2021; Lin and Shei, 2008). There is still limited understanding about the
61 inhibitory mechanisms of Cu on fermentative hydrogen production, especially about
62 the microbiological mechanism. As a biological process, microbes in the reactor and
63 their related functional genes essentially determine the metabolic pathway and activity
64 of fermentative H_2 production (Cai et al., 2011). Accordingly, the impact of Cu on the
65 microbial community structure and functional genes in dark hydrogen fermentation
66 requires to be further investigated.
67 Therefore, the present study aimed to explore the inhibitory mechanisms of Cu
68 on dark hydrogen fermentation. First, the influence of different concentrations of Cu
69 on the fermentation performances, including hydrogen yield, glucose utilization and

liquid metabolites formation, were experimentally investigated. Second, the impact of Cu on the bacterial community structure and functional genes associated with key hydrogen-producing pathways were analyzed to elucidate the related inhibition mechanisms. This study will facilitate the ability to understand how heavy metals inhibit the process efficiency of dark fermentation, and provide theoretical guidance for mitigating the inhibition effect.

2. Materials and methods

2.1. Inoculum preparation

In the present work, the seed sludge (i.e. anaerobically digested sludge) was collected from a local wastewater treatment plant. The main properties of the raw seed sludge were: TS content, 54.33 g/L; volatile solids (VS) content, 27.91 g/L; and pH= 6.80. The raw seed sludge was heated to 100 °C and maintained there for fifteen minutes to eliminate hydrogen-consuming microorganisms (Yang and Wang, 2021). After cooling to the ambient temperature, the pretreated sludge was centrifuged and washed via resuspension using deionized water (Cao et al., 2022), and then was used as the fermentation inoculum. VS concentration of the inoculum used was 16.67 g/L, and the dominant genera in the inoculum were *Clostridium sensu stricto*, *Proteiniphilum*, *Petrimonas*, *Candidatus Caldatribacterium*, *Sedimentibacter* and *Paraclostridium*.

2.2. Batch fermentation experiments

Batch H_2 fermentation experiments were conducted in triplicate using a series of 150 mL glass bottles, including 10 mL nutrients solution (without Cu), 30 mL inoculum, 60 mL deionized water, and 1 g glucose. Each liter of nutrients solution

contained 0.004 g $NiCl_2 \cdot 6H_2O$, 0.085 g $MgCl_2 \cdot 6H_2O$, 0.25 g $FeSO_4 \cdot 7H_2O$, 5 g $K_2HPO_4 \cdot 3H_2O$, 5 g $NaH_2PO_4 \cdot 2H_2O$, 5 g NH_4Cl and 40 g $NaHCO_3$ (Yang et al., 2019). Cu concentrations in the reactors were set by adding $CuCl_2$ (99.9%, Macklin Biochemical Co., Ltd) at 5, 10, 100, 500, and 1000 mg/L, which were named as the Cu-5, Cu-10, Cu-100, Cu-500, and Cu-1000 groups, respectively. The group without Cu addition was set as the control. The initial pH of the mixture in all reactors was adjusted to 7.00 ± 0.10. Finally, all reactors were flushed with nitrogen gas, and then placed in a shaker (120 rpm) at 37 °C for biohydrogen production.

2.3. Bacterial community analysis

When the fermentation process terminated, samples of the control group and the groups with significant lower hydrogen yield induced by Cu^{2+} were collected to study the impact of Cu^{2+} on bacterial community structure. The FastDNA SPIN Kit for soil was used in this work for DNA extraction. PCR amplification of the V4-V5 region of bacterial 16S rRNA gene was conducted with the primers 515F/907R (Yang and Wang, 2021). After PCR purification and qualification, the sequencing of PCR amplicons was conducted, and the Operational Units (OTUs) were clustered at an identity threshold of 97%. In order to obtain the bacterial community composition, taxonomic assignment of the OTUs was carried out using RDP Classifier against the Silva database. Bacterial alpha diversity was evaluated by the Shannon index in this work, which referred to the variety of different species of bacteria present in a fermentation sample (Lozupone and Knight, 2008). Bacterial richness was evaluated by the indices of ACE and Chao1 in this work, which referred to the total number of bacterial species present in a fermentation sample (Lozupone and Knight, 2008).

2.4. Metagenomic analysis

In this work, the control group and the Cu-1000 group were selected for metagenomic sequencing. The DNA extraction approach was the same as that used in the bacterial community analysis. After the construction of paired-end library, the sequence was performed on an Illumina HiSeq 2000 platform. The clean reads of the genome dataset were assembled into contigs (length >= 300 bp), which were then uploaded and used for gene prediction and annotation. The KEGG annotation were obtained by aligning representative sequences to the Kyoto Encyclopedia of Genes and Genomes database using BLAST with e-value cutoff of $1e^{-5}$ (Zhu et al., 2022). The abundances of the genes were calculated based on the reads per kilobase per million mapped reads (RPKM) (Tang et al., 2022).

2.5. Other analytical methods

TS and VS concentrations of the seed sludge were analyzed according to the APHA standard methods (APHA, 2005). In detail, 10.0 mL of the sludge sample was dried until a constant weight at 105 °C to determine the TS concentration, and then the dried sludge sample was calcined at 600 °C in a muffle furnace until a constant weight to determine the VS concentration. After filtering the fermentation broth through a membrane (0.45 μm), glucose and the dominant liquid metabolic products (acetate, propionate and butyrate) were analyzed using a high-performance liquid chromatography (Cao et al., 2022). Glucose utilization efficiency was calculated according to Eq. (1) at the end of the hydrogen fermentation.

$$\text{Glucose utilization efficiency (\%)} = (Glu_{initial}\text{-}Glu_{end})/Glu_{initial} \quad (1)$$

Where, $Glu_{initial}$ was defined as the glucose concentration before the start-up of hydrogen fermentation; Glu_{end} was defined as the glucose concentration at the end of hydrogen fermentation.

Total volume of the produced biogas for all reactors was determined by water displacement method. The fraction of hydrogen in biogas was determined by a gas chromatography with carrier gas of helium (80 mL/min) (Wang et al., 2022). Operational temperatures of the gas chromatography were: injection port, 120°C; column oven, 110°C; and detector, 150 °C. The modified Gompertz model was employed to fit the cumulative H_2 production data in this work (Yang et al., 2019).

3. Results and discussion

3.1. The influence of Cu^{2+} on hydrogen production

The impact of different concentrations of Cu^{2+} on cumulative hydrogen production is shown in Fig. 1. For all six groups, the hydrogen-producing process completed within 48 h, and followed the same pattern of lag, rapid and slow phases. The similar H_2-producing pattern has also been found in other fermentation reactors (Kim et al., 2022; Matyakubov et al., 2022).

Fig. 1

The modified Gompertz model was employed to evaluate the hydrogen fermentation characteristics by fitting the data in Fig. 1 ($R^2 > 0.99$) (Table 1). For the cumulative hydrogen production potential (P), the value decreased slightly at Cu^{2+} concentrations of lower than 100 mg/L, while decreased significantly at Cu^{2+} concentrations of higher than 500 mg/L, indicating that the high concentrations of Cu^{2+} reduced the hydrogen-producing capacity of fermentative bacteria. For the

maximum hydrogen production rate (R_m), the control group obtained the highest value, reaching 24.51 mL/h. Upon exposure to Cu^{2+}, R_m showed a deceasing trend with the increasing Cu^{2+} concentration. The lowest R_m was only 2.05 mL/h for the Cu-1000 group, which was reduced by 91.64% as compared with the group without Cu^{2+} addition. The decline in P and R_m values may be attributed to that those high concentrations of Cu^{2+} decreased the activity of vital enzymes involved in H_2 generation and inhibited the growth of biohydrogen-producing microbes (Chen et al., 2021). For the lag time (λ), it is evident that the low concentrations of Cu^{2+} (<= 100 mg/L) shortened the lag time for hydrogen production, while the higher concentrations of Cu^{2+} (>= 500 mg/L) prolonged the lag time. Possible reason for this phenomenon is that Cu^{2+} at a low concentration can function as a trace growth factor for biohydrogen-producing bacteria (Sharma and Melkania, 2018), which shortened the time to recover microbial activity after the high temperature pretreatment, while excessive amount of Cu^{2+} was toxic to biohydrogen-producing bacteria (Wong et al., 2014), thereby restricting the recovery of microbial activity for biohydrogen production during the initial phase of the fermentation.

Table 1

When the fermentation process terminated, the control group obtained the highest hydrogen yield value, reaching 1.49 mol H_2/mol-glucose. This value of hydrogen yield is within the normal range of the values obtained by literature (Yang et al., 2019; Wang and Yin, 2017). With the exposure to Cu^{2+} at 5, 10, 100, 500 and 1000 mg/L, the hydrogen yields decreased to 1.44, 1.37, 1.33, 0.59 and 0.05 mol H_2/mol-glucose, respectively. It is clear that Cu^{2+} exposure inhibited the fermentative

hydrogen production, especially when the exposure concentration of Cu^{2+} was higher than 500 mg/L (Student's *t*-test, $p<0.05$). The inhibition in hydrogen production may be due to that the high concentrations of Cu^{2+} caused the increased generation of reactive oxygen species (ROS) in bacterial cells, then leading to DNA damage and the decline of enzymatic activity (Chen et al., 2021). In addition, the exposure to higher concentrations of Cu can destroy the integrity of cytoplasmic membrane and inhibit the uptake of essential nutrients during the cultivation of bacteria (Lemire et al., 2013). These adverse effects may cause the growth arrest of fermentative bacteria, or even lead to the death of some high-yielding biohydrogen-producing microbes, thereby decreasing the values of hydrogen yield. Similarly, Sharma and Melkania (2018) found that H_2 production of dark fermentation decreased from 226.9 to 153.8 mL upon exposure to Cu^{2+} at 100 mg/L. The different inhibition threshold between Sharma and Melkania (2018) and this study may be due to different bacterial community in the inoculum.

3.2. Glucose utilization and liquid metabolites formation

Besides hydrogen production, glucose utilization efficiency is also an important aspect for assessing the fermentation performance in this work. Fig. 2 shows the influence of Cu^{2+} on the utilization efficiencies of glucose. It can be seen that the glucose utilization efficiency was 97.49% for the control group, and it changed barely at the Cu^{2+} concentrations of lower than 100 mg/L (97.44-97.55%). However, the glucose utilization efficiency declined significantly at the Cu^{2+} concentrations of higher than 500 mg/L, probably because the high concentrations of Cu^{2+} decreased the activities of microbes and functional enzymes (e.g. glucokinase, pyruvate

decarboxylase and glucose-6-phosphate dehydrogenase). The decreased efficiency of glucose utilization may cause the decline of hydrogen production for the Cu-500 and Cu-1000 groups.

Fig. 2

The main liquid metabolites generated from glucose utilization were further analyzed (Fig. 3), which could be used as an indicator to deduce the metabolic pathways of fermentative microbes. As shown in Fig. 3, the concentration of total metabolites (acetate, butyrate and propionate) was 4238.89 mg/L in the fermenter without Cu^{2+} addition, and decreased by 7.15%, 11.43%, 11.90%, 48.11% and 89.40% upon the exposure to Cu^{2+} at 5, 10, 100, 500 and 1000 mg/L, respectively. Particularly, acetate and butyrate concentrations significantly decreased at Cu^{2+} of higher than 500 mg/L. During dark fermentation, these two metabolites are commonly formed in the H_2-producing pathways (Hallenbeck, 2009). Much lower concentrations of acetate and butyrate in the Cu-500 and Cu-1000 systems indicate the significant lower yield of hydrogen, which can be confirmed in Fig. 1.

Fig. 3

Regarding the composition of these metabolites, acetate and butyrate were the major components in the control, Cu-5, Cu-10, Cu-100 and Cu-500 fermenters, with acetate proportions of 60.13%, 63.73%, 61.62%, 66.85% and 44.16%, and butyrate proportions of 39.87%, 36.23%, 38.31%, 33.01% and 55.75%, respectively, which indicated that the butyrate-type fermentation dominated in the aforementioned five fermenters. Nevertheless, the mixed-acid type fermentation played a dominant role in the Cu-1000 fermener, with butyrate and propionate proportions of 87.51% and

12.49%, respectively. This phenomenon may be due to that such a high concentration of Cu^{2+} changed the bacterial community structure, thereby leading to a shift in the metabolic pathway during the fermentation process. Other studies also found that the exposure to Cu^{2+} changed the fermentation type of biohydrogen production (Lin and Shei, 2008; Han et al., 2014).

3.3. Bacterial community analysis

Bacterial communities present in the system play a crucial role in the efficiency of a dark fermentation bioreactor (Hung et al., 2011). In order to understand how Cu^{2+} inhibited the hydrogen productivity, bacterial community structures of the control, Cu-500 and Cu-1000 groups were analyzed and compared in this study. Table 2 shows the indices of bacterial diversity and richness for the aforementioned three groups.

Table 2

As illustrated in Table 2, the Good's coverage values were higher than 0.999 for all three samples, indicating that the sequencing depth was enough to capture adequate bacterial community. The value of Shannon index follows the order of control > Cu-500 > Cu-1000, which indicates that the exposure to high concentrations of Cu^{2+} decreased the bacterial diversity during the fermentation process. Meanwhile, as compared to the Cu-500 and Cu-1000 samples, the control sample also exhibited higher values of Chao1 and Ace (Table 2), indicating that high concentrations of Cu^{2+} also decreased the bacterial richness. The decline in bacterial diversity and richness may be attributed to that the excessive Cu^{2+} was toxic to fermentative bacteria in the inoculum, thereby leading to the death of some bacterial species during the

252 fermentation process. The loss of some types of functional bacteria (e.g.
253 *Paraclostridium*, *Clostridium sensu stricto* 1 and *Clostridium sensu stricto* 18) may
254 lead to the decline in hydrogen yield for the Cu-500 and Cu-1000 systems.
255 Furthermore, bacterial compositions at genus level for the control, Cu-500 and
256 Cu-1000 groups were compared and illustrated in Fig. 4. According to Fig. 4, high
257 concentrations of Cu^{2+} remarkably changed the bacterial community structure in
258 hydrogen fermentation. For the control reactor, the genera *Clostridium sensu stricto*
259 were dominant with a relative abundance of 73.79%, followed by *Paraclostridium*
260 (15.37%), and *Bacillus* (4.45%). For the Cu-500 system, *Bacillus* became dominant
261 with relative abundance of 86.06%, while the abundance of genera *Clostridium sensu*
262 *stricto* was dramatically reduced to 10.12%. When increasing the Cu^{2+} concentration
263 to 1000 mg/L, the abundance of the genera *Clostridium sensu stricto* further
264 decreased to 0.29%, and *Bacillus* became the only dominant genus with relative
265 abundance of 98.69%. It is clear that the exposure to high concentrations of Cu^{2+}
266 significantly inhibited the growth of *Clostridium sensu stricto* during the fermentation
267 process, which might be the determinant reason for the declined biohydrogen
268 production for the Cu-500 and Cu-1000 groups. It has been found that *Clostridium*
269 *sensu stricto* genera are highly-yielding H_2 producers in dark fermentation system,
270 which can use multiple substances (e.g. starch, sucrose and glucose) to produce
271 hydrogen (Mo et al., 2022). Meanwhile, *Clostridium sensu stricto* have a theoretical
272 hydrogen production of 4 mol H_2/mol glucose (Hallenbeck, 2009), which is much
273 higher than that of other biohydrogen-producing genera, like *Enterobacter* and
274 *Bacillus* (Wang and Yin, 2017). Similarly, other investigations also observed a

significant positive correlation between hydrogen yield and *Clostridium sensu stricto* genera in dark fermentation (Yang and Wang, 2021; Li et al., 2020; Zhao et al., 2020).

Fig. 4

In addition, the relative abundance of genus *Paraclostridium* also significantly decreased upon exposure to high concentrations of Cu^{2+}. *Paraclostridium* belongs to obligate anaerobe that can use glucose for fermentative H_2 production (Sasi Jyothsna et al., 2016; Yang et al., 2019). Therefore, the much lower *Paraclostridium* abundance may be another factor leading to the lower hydrogen yield for the Cu-500 and Cu-1000 systems. By contrary, the abundance of *Bacillus* significantly increased upon exposure to Cu^{2+} at 500 and 1000 mg/L, indicating that this genus was more resist to Cu^{2+} compared to the other genera, probably due to its better spore-forming ability (Hawkes et al., 2002). Although it has been reported that several species of *Bacillus* are H_2-producing bacteria (Kumar et al., 2015; Ramu et al., 2020), their hydrogen productivity is commonly lower than that of *Clostridium* spp. (Wang and Yin, 2017). Meanwhile, because hydrogen yield of the Cu-1000 group was only 0.05 mol H_2/mol-glucose, it can be inferred that *Bacillus* species enriched in this study were not hydrogen producers.

3.4. Metagenomic analysis of functional genes involved in hydrogen production

Functional genes in active bacteria fundamentally determine the metabolic pathway and activity in dark fermentation bioreactor (Jiang et al., 2021). Accordingly, metagenomic analysis was employed to compare the metabolic functions between the

control fermenter and the Cu-1000 fermenter based on the KEGG database, and the findings are shown in Fig. 5.

Fig. 5

According to Fig. 5, the relative abundances of sequences related to both glycolysis and pyruvate metabolism were significantly higher in the control system compared with the Cu-1000 system, indicating that glycolysis and pyruvate metabolism were significantly inhibited with exposure to the high concentration of Cu^{2+}. These two processes are crucial for converting glucose to hydrogen during the dark fermentation process. Therefore, as compared with the control group, the inhibition on these two metabolic processes may cause the significant lower hydrogen yield for the Cu-1000 group. In general, glucose is firstly transported into cells, and then break down into intermediate pyruvate, NADH and ATP through glycolysis. Afterwards, there are three possible pathways to produce H_2 (Fig. 6a) (Hallenbeck, 2009). For the first pathway, intermediate pyruvate is broken down into acetyl-CoA and formate, which is further decomposed to H_2 and CO_2. For the second pathway, reduced ferredoxin, which is generated during the decomposition of intermediate pyruvate into acetyl-CoA and CO_2, transfers electrons to hydrogenase, finally generating H_2. For the third pathway, the reduced NADH, which is generated from glycolysis, can be re-oxidized with proton reduction to produce H_2. The metabolic activity of the aforementioned three pathways primarily relies on biochemical reactions catalyzed by functional enzymes, so the abundances of genes encoding these functional enzymes were further investigated (Fig. 6b).

Fig. 6

The membrane transport of glucose into bacterial cells is the first stage for biohydrogen production. It is apparent in Fig. 6b that the genes related to glucose transport, including *gtsA* (K17315), *gtsB* (K17316) and *gtsC* (K17317) (No. 1-3), were significantly down-regulated in the presence of high concentration of Cu^{2+}, with the abundances decreasing by 84.74%, 76.56% and 69.10% in comparison with the control, respectively. This phenomenon indicates that the exposure to high concentrations of Cu^{2+} inhibited the membrane transport of glucose into bacterial cells, thereby blocking the intracellular metabolite of glucose for producing hydrogen from the source.

When glucose is delivered into bacterial cells, the glucose will be further converted to pyruvate, reduced NADH, and ATP through glycolysis. The impact of Cu^{2+} on the genes encoding the enzymes involved in glycolysis (No. 4-18) is illustrated in Fig. 6b. For instance, in the presence of 1000 mg/L Cu^{2+}, the abundances of genes encoding pyruvate kinase (K00873, *PK*), hexokinase (K00844, *HK*), polyphosphate glucokinase (K00886, *ppgK*), glucose-6-phosphate isomerase (K13810, *tal-pgi*), ATP-dependent phosphofructokinase (K21071, *pfk*), ADP-dependent phosphofructokinase (K00918, *pfkC*), fructose 1,6-bisphosphate aldolase (K01622, *K01622*), phosphoglycerate kinase (K00927, *PGK*), 2,3-bisphosphoglycerate-independent phosphoglycerate mutase (K15635, *apgM*) and enolase (K01689, *ENO*) decreased by 61.79%, 70.68%, 76.30%, 78.18%, 85.60%, 70.00%, 73.22%, 35.93%, 74.37% and 35.94% in comparison with the control, respectively. This phenomenon indicates that the high concentration of Cu^{2+} significantly inhibited the synthesis of enzymes to break down glucose into pyruvate

and reduced NADH, thereby resulting in much less precursors for the subsequent hydrogen production.

The abundances of genes involved in hydrogen formation were further analyzed in detail (Fig. 6b). As shown in Fig. 6b, with exposure to the high concentration of Cu^{2+}, the relative abundances of genes encoding formate C-acetyltransferase (K00656, *E2.3.1.54*) (No. 21) and pyruvate formate lyase activating enzyme (K04069, *pflA*) (No. 22), which play important roles on the decomposition of pyruvate into formate, decreased by 73.69% and 80.81% in comparison with the control, respectively. Meanwhile, the abundance of gene encoding formate dehydrogenase major subunit (K00123, *fdoG*) (No. 23), which acts on the decomposition of formate to hydrogen and CO_2, decreased by 72.31% upon exposure to the high concentration of Cu^{2+}. The down-regulation of the aforementioned three genes was disadvantageous to hydrogen production from the "formate-decomposition pathway". In addition, the abundances of genes encoding pyruvate-ferredoxin oxidoreductase (K03737, *por*) (No. 19) and ferredoxin hydrogenase (K00532, *E1.12.7.2*) (No. 20) significantly decreased from 291.02 and 35.07 RPKM to 50.34 and 0 RPKM with exposure to the high concentration of Cu^{2+}, respectively. As the genes *por* and *E1.12.7.2* play crucial roles in the other two biohydrogen-producing pathways (i.e. "the NADH−oxidation pathway" and "the pyruvate-decomposition pathway"), the down-regulation of these genes were also unfavorable for hydrogen production. In summary, the high concentration of Cu^{2+} significantly down-regulated the abundances of functional genes related to three biohydrogen-producing pathways, which was the fundamental factor leading to the significant low hydrogen yield for the Cu-1000 group.

In addition, as shown in Fig. 6b, the relative abundances of genes encoding phosphate acetyltransferase (K13788, *pta*) (No. 24), acetate kinase (K00925, *ackA*) (No. 25), butyryl-CoA dehydrogenase (K00248, *ACADS*) (No. 26), phosphate butyryltransferase (K00634, *ptb*) (No. 27) and butyrate kinase (K00929, *buk*) (No. 28), which contribute to the formation of acetate (No. 24-25) and butyrate (No. 26-28), were all remarkably decreased with exposure to the high concentration of Cu^{2+}. The down-regulation of these genes may contribute to the much lower yield of acetate and butyrate for the Cu-1000 group.

3.5. Implications to fermentative hydrogen production

As a typical heavy metal that has been widely detected in the feedstocks of dark fermentation, Cu can inhibit the hydrogen production efficiency. Previous investigations mainly concentrated on the inhibition effect of Cu on dark fermentation performances (e.g. hydrogen yield and substrate utilization) (Li and Fang, 2007; Lin and Shei, 2008; Mohanraj et al., 2016), while current understanding on the inhibitory mechanisms of Cu on dark fermentation is still lacking. This work investigated the inhibitory mechanisms of Cu on dark fermentation from the aspects of bacterial community structure and functional genes for filling the existing knowledge gap.

In addition to bacterial community structure and functional genes, the activity of key enzymes also plays an important role in fermentative hydrogen production (Hallenbeck, 2009). In future work, it is suggested to investigate the impact of Cu on the activity of some key enzymes (e.g. pyruvate kinase, pyruvate-ferredoxin oxidoreductase and hydrogenase) involved in hydrogen production. Furthermore, the strategies for relieving the inhibition of Cu on dark fermentation should also be

considered. For instance, the co-fermentation of high-Cu feedstocks (e.g. sewage sludge and livestock manure) with low-Cu feedstocks (e.g. potato peel waste and macroalgae) may be a promising approach for mitigating the inhibition effect of Cu on fermentative hydrogen production.

4. Conclusions

Cu^{2+} significantly inhibited fermentative hydrogen production at exposure concentrations of higher than 500 mg/L. High concentrations of Cu^{2+} also reduced the hydrogen production rate, prolonged the hydrogen-producing lag phase, and inhibited the liquid metabolites formation. Mechanisms analysis showed that the presence of high concentrations of Cu^{2+} significantly declined the utilization efficiency of glucose, led to much less enrichment of high-yielding hydrogen-producing genera (e.g. *Clostridium sensu stricto*), and remarkably down-regulated the abundances of genes involved in glycolysis (e.g. *PK*, *ppgK* and *pgi-pmi*) and hydrogen formation (e.g. *pflA*, *fdoG*, *por* and *E1.12.7.2*), fundamentally leading to the inhibition on the fermentation efficiency.

Acknowledgements

This study was supported by the National Natural Science Foundation of China (No. 41991332), the Key Research and Development Program of Shandong Province, China (No. 2021CXGC010803), and the China Postdoctoral Science Foundation (No. 2022M713307).

References

1. Al-Saydeh, S.A., El-Naas, M.H., Zaidi, S.J., 2017. Copper removal from industrial wastewater: A comprehensive review. J. Ind. Eng. Chem. 56, 35–44.
2. APHA, 2005. Standard Methods for the Examination of Water and Wastewater, twenty first ed. American Public Health Association/American Water Works Association/Water Environment Federation, Washington, DC, USA.
3. Arun, J., Sasipraba, T., Gopinath, K.P., Priyadharsini, P., Nachiappan, S., Nirmala, N., Dawn, S.S., Chi, N.T.L., Pugazhendhi, A., 2022. Influence of biomass and nanoadditives in dark fermentation for enriched bio-hydrogen production: A detailed mechanistic review on pathway and commercialization challenges. Fuel 327, 125112.
4. Bundhoo, M.Z., Mohee, R., 2016. Inhibition of dark fermentative bio-hydrogen production: a review. Int. J. Hydrogen Energy, 41, 6713-6733.
5. Cai, G.Q., Jin, B., Monis, P., Saint, C., 2011. Metabolic flux network and analysis of fermentative hydrogen production. Biotechnol. Adv. 29, 375–387.
6. Cao, J.M., Xu, C.L., Zhou, R., Duan, G.L., Lin, A.J., Yang, X., You, S., Zhou, Y.Y., Yang, G., 2022. Potato peel waste for fermentative biohydrogen production using different pretreated culture. Bioresour. Technol. 362, 127866.
7. Cheng, D.L., Ngo, H.H., Guo, W.S., Chang, S.W., Nguyen, D.D., Deng, L.J., Chen Z., Ye, Y.Y., Bui, X.T., Hoang, N.B., 2022. Advanced strategies for

enhancing dark fermentative biohydrogen production from biowaste towards sustainable environment. Bioresour. Technol. 351, 127045.

8. Chen, Y., Yin, Y.N., Wang, J.L., 2021. Recent advance in inhibition of dark fermentative hydrogen production. Int. J. Hydrogen Energy 46, 5053–5073.

9. Chu, L.Q., He, W., 2021. Toxic metals in soil due to the land application of sewage sludge in China: Spatiotemporal variations and influencing factors. Sci. Total Environ. 757, 143813.

10. Dahiya, S., Chatterjee, S., Sarkar, O., Mohan, S.V., 2021. Renewable hydrogen production by dark-fermentation: Current status, challenges and perspectives. Bioresour. Technol. 321, 124354.

11. Elbeshbishy, E., Dhar, B.R., Nakhla, G., Lee, H.S., 2017. A critical review on inhibition of dark biohydrogen fermentation. Renew. Sustain. Energy Rev. 79, 656-668.

12. Fan, X.N., Li, Y.M., Luo, Z.Y., Jiao, Y.G., Ai, F., Zhang, H.R., Zhu, S.N., Zhang, Q.G., Zhang, Z.P., 2022. Surfactant assisted microwave irradiation pretreatment of corncob: Effect on hydrogen production capacity, energy consumption and physiochemical structure. Bioresour. Technol. 357, 127302.

13. Guan, T.X., He, H.B., Zhang, X.D., Bai, Z., 2011. Cu fractions, mobility and bioavailability in soil-wheat system after Cu-enriched livestock manure applications. Chemosphere 82, 215–222.

14. Gujre, N., Rangan, L., Mitra, S., 2021. Occurrence, geochemical fraction, ecological and health risk assessment of cadmium, copper and nickel in soils contaminated with municipal solid wastes. Chemosphere 271, 129573.
15. Hallenbeck, P.C., 2009. Fermentative hydrogen production: Principles, progress, and prognosis. Int. J. Hydrogen Energy 34, 7379–7389.
16. Han, H.L., Jia, Q.B., Wei, L.L., Shen, J.Q., 2014. Influence of Cu^{2+} concentration on the biohydrogen production of continuous stirred tank reactor. Int. J. Hydrogen Energy 39, 13437–13442.
17. Hawkes, F.R., Dinsdale, R., Hawkes, D.L., Hussy, I., 2002. Sustainable fermentative hydrogen production: challenges for process optimisation. Int. J. Hydrogen Energy 27, 1339-1347.
18. Hung, C.H., Chang, Y.T., Chang, Y.J., 2011. Roles of microorganisms other than *Clostridium* and *Enterobacter* in anaerobic fermentative biohydrogen production systems – A review. Bioresour. Technol. 102, 8437–8444.
19. Jiang, X.P., Yan, Y.Y., Feng, L.Y., Wang, F., Guo, Y.Q., Zhang, X.Z., Zhang, Z.G., 2021. Bisphenol A alters volatile fatty acids accumulation during sludge anaerobic fermentation by affecting amino acid metabolism, material transport and carbohydrate-active enzymes. Bioresour. Technol. 323, 124588.
20. Kim, B., Jeong, J., Kim, J., Yoon, H.H., Nguyen, P.K.T., Kim, J., 2022. Mathematical modeling of dark fermentation of macroalgae for hydrogen and volatile fatty acids production. Bioresour. Technol. 354, 127193.

21. Kumar, P., Sharma, R., Ray, S., Mehariya, S., Patel, S.K.S., Lee, J.K., Kalia, V.C., 2015. Dark fermentative bioconversion of glycerol to hydrogen by *Bacillus thuringiensis*. Bioresour. Technol. 182, 383–388.
22. Khoufi, S., Louhichi, A., Sayadi, S., 2015. Optimization of anaerobic co-digestion of olive mill wastewater and liquid poultry manure in batch condition and semi-continuous jet-loop reactor. Bioresour. Technol. 182, 67-74.
23. Lemire, J.A., Harrison, J.J., Turner, R.J., 2013. Antimicrobial activity of metals: mechanisms, molecular targets and applications. Nat. Rev. Microbiol. 11, 371–384.
24. Li, C., Fang, H.H.P., 2007. Inhibition of heavy metals on fermentative hydrogen production by granular sludge. Chemosphere 67, 668–673.
25. Li, H., Song, W.L., Cheng, J., Ding, L.K., Zhou, J.H., Li, Y.Y., 2020. Effects of harvest month on biochemical composition of alligator weed for biohydrogen and biomethane cogeneration：Identifying critical variations in microbial communities. Int. J. Hydrog. Energy 45, 4161–4173.
26. Lin, C.Y., Shei, S.H., 2008. Heavy metal effects on fermentative hydrogen production using natural mixed microflora. Int. J. Hydrogen Energy 33, 587–593.
27. Liu, W.R., Zeng, D., She, L., Su, W.X., He, D.C., Wu, G.Y., Ma, X.R., Jiang, S., Jiang, C.H., Ying, G.G., 2020. Comparisons of pollution characteristics, emission situations, and mass loads for heavy metals in the manures of different livestock and poultry in China. Sci. Total Environ. 734, 139023.

28. Lozupone, C.A., Knight, R., 2008. Species divergence and the measurement of microbial diversity. FEM Microbiol. Rev. 32, 557-578.

29. Martínez-Mendoza, L.J., Lebrero, R., Muñoz, R., García-Depraect, O., 2022. Influence of key operational parameters on biohydrogen production from fruit and vegetable waste via lactate-driven dark fermentation. Bioresour. Technol. 364, 128070.

30. Matyakubov, B., Hwang, Y., Lee, T.J., 2022. Evaluating interactive toxic impact of heavy metals and variations of microbial community during fermentative hydrogen production. Int. J. Hydrogen Energy 47, 31223–31240.

31. Mo, H., Wang, N., Ma, Z.M, Zhang, J.S., Zhang, J.L., Wang, L., Dong, W.F., Zang, L.H., 2022. Hydroxyapatite fabrication for enhancing biohydrogen production from glucose dark fermentation. ACS omega, 7, 10550-10558.

32. Ramu, S.M., Thulasinathan, B., Hari, D.G., Bora, A., Jayabalan, T., Mohammed, S.N., Doble, M., Arivalagan, P., Alagarsamy, A., 2020. Fermentative hydrogen production and bioelectricity generation from food based industrial waste: An integrative approach. Bioresour. Technol. 310, 123447.

33. Ren, Y., Si, B.C., Liu, Z.D., Jiang, W.Z., Zhang, Y.H., 2022. Promoting dark fermentation for biohydrogen production: Potential roles of iron-based additives. Int. J. Hydrogen Energy 47, 1499–1515.

34. Sasi Jyothsna, T.S., Tushar, L., Sasikala, C., Ramana, C.V. 2016. *Paraclostridium benzoelyticum* gen. nov., sp. nov., isolated from marine sediment

and reclassification of *Clostridium bifermentans* as *Paraclostridium bifermentans* comb. nov. Proposal of a new genus *Paeniclostridium* gen. nov. to accommodate *Clostridium sordellii* and *Clostridium ghonii*. Int. J. Syst. Evol. Microbiol. 66, 1268–1274.

35. Sharma, P., Melkania, U., 2018. Impact of heavy metals on hydrogen production from organic fraction of municipal solid waste using co-culture of *Enterobacter aerogenes* and *E. Coli*. Waste Manag. 75, 289–296.
36. Sillero, L., Solera, R., Perez, M., 2022. Anaerobic co-digestion of sewage sludge, wine vinasse and poultry manure for bio-hydrogen production. Int. J. Hydrogen Energy 47, 3667-3678.
37. Sivagurunathan, P., Sen, B., Lin, C.Y., 2015. High-rate fermentative hydrogen production from beverage wastewater. Appl. Energy 147, 1–9.
38. Tang, X., Zhou, M., Zeng, G.M., Fan, C.Z., 2022. The effects of dimethyl phthalate on sludge anaerobic digestion unveiling the potential contribution of plastic chemical additive to spread of antibiotic resistance genes. Chem. Eng. J. 435, 134734.
39. Urrutia, C., Yañez-Mansilla, E., Jeison, D., 2019. Bioremoval of heavy metals from metal mine tailings water using microalgae biomass. Algal Res. 43, 101659.
40. Wang, J.L., Yin, Y.N., 2017. Principle and application of different pretreatment methods for enriching hydrogen-producing bacteria from mixed cultures. Int. J. Hydrogen Energy 42, 4804–4823.

41. Wang, Q.Y., Fu, H., Zhang, G.M., Wu, Y., Ma, W.F., Fu, C., Cai, Y.J., Zhong, L.H., Zhao, Y.W., Wang, X.Y., Zhang, P.Y., 2022. Efficient chain elongation synthesis of n-caproate from shunting fermentation of food waste. Bioresour. Technol. 128569.

42. Wong, Y.M., Wu, T.Y., Juan, J.C., 2014. A review of sustainable hydrogen production using seed sludge via dark fermentation. Renew. Sustain. Energy Rev. 34, 471-482.

43. Yang, G., Wang, J.L., 2021. Biohydrogen production by co-fermentation of antibiotic fermentation residue and fallen leaves: Insights into the microbial community and functional genes. Bioresour. Technol. 337, 125380.

44. Yang, G., Yin, Y.N., Wang, J.L., 2019. Microbial community diversity during fermentative hydrogen production inoculating various pretreated cultures. Int. J. Hydrogen Energy 44, 13147–13156.

45. Zhao, W.Q., Zhang, J.S., Zhang, H.W., Yang, M.C., Zang, L.H., 2020. Comparison of mesophilic and thermophilic biohydrogen production amended by nickel-doped magnetic carbon. J. Clean. Prod. 270, 122730.

46. Zhu, D., Ma, J., Li, G., Rillig, M.C., Zhu, Y.G., 2022. Soil plastispheres as hotspots of antibiotic resistance genes and potential pathogens. ISME J. 16, 521-532.

Figure Captions

Fig. 1 The influence of Cu^{2+} on cumulative hydrogen production during the fermentation process

Fig. 2 The impact of Cu^{2+} on glucose utilization after the hydrogen fermentation

Fig. 3 The impact of Cu^{2+} on liquid metabolites concentrations after the fermentation

Fig. 4 Bacterial community compositions for the control, Cu-500 and Cu-1000 groups at genus level

Fig. 5 Comparison of metabolic functions for the control group and Cu-1000 group using the KEGG database at level 3

Fig. 6 Principle metabolic pathways of fermentative hydrogen production (a); The impact of Cu^{2+} on the abundances of functional genes associated with biohydrogen production as detected by metagenomics sequencing (b)

Tables

Table 1 Kinetic analysis for hydrogen fermentation with different concentrations of Cu^{2+}

Model	Parameters	Cu^{2+} concentration (mg/L)					
		0	5	10	100	500	1000
Modified Gompertz	P (mL)	187.57	181.14	171.57	168.26	76.18	6.01
	R_m (mL/h)	24.51	17.02	14.10	12.65	3.36	2.05
	λ (h)	11.83	9.65	9.68	9.24	18.79	21.03
	R^2	0.990	0.990	0.996	0.994	0.996	0.999

Table 2 Bacterial diversity and richness indices for the control, Cu-500 and Cu-1000 samples

Sample	Clean reads	Coverage	Shannon	Ace	Chao1
Control	106210	0.999	1.85	325.89	334.32
Cu-500	135228	0.999	0.83	317.58	301.55
Cu-1000	145261	0.999	0.75	226.80	218.89

Figures

Fig. 1

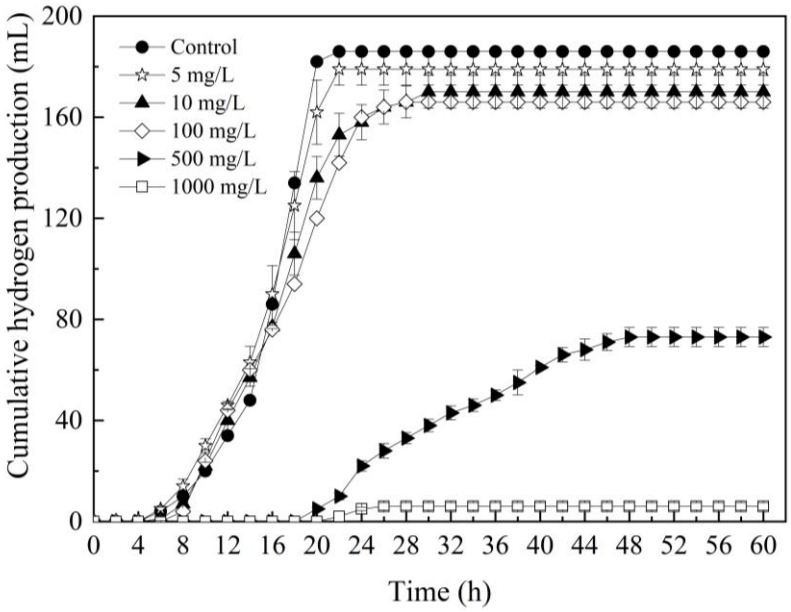

Fig. 2

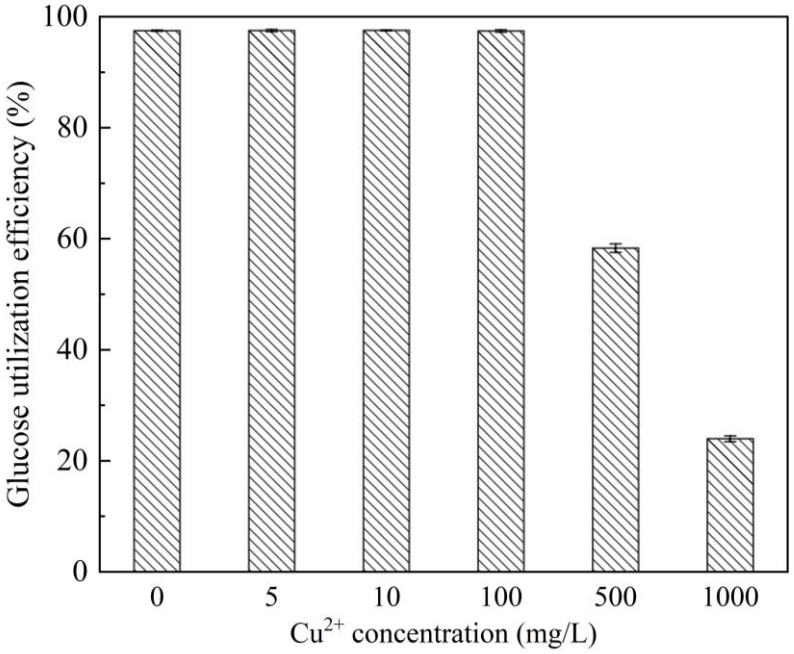
Glucose utilization efficiency (%)
100
80
60
40
20
0
0
5
10
100
500
1000
Cu2+ concentration (mg/L)

Fig. 3

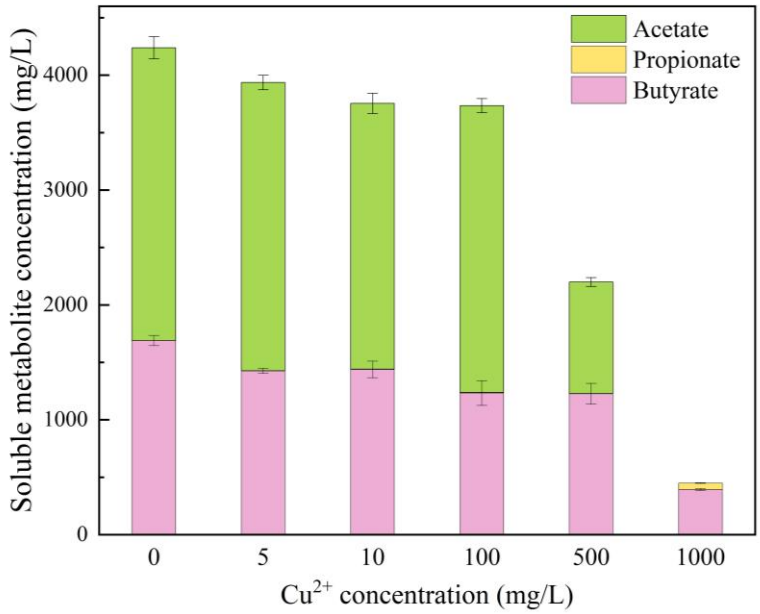
Acetate
Propionate
Butyrate
Soluble metabolite concentration (mg/L)
0
1000
2000
3000
4000
0
5
10
100
500
1000
Cu2+ concentration (mg/L)

Fig. 4

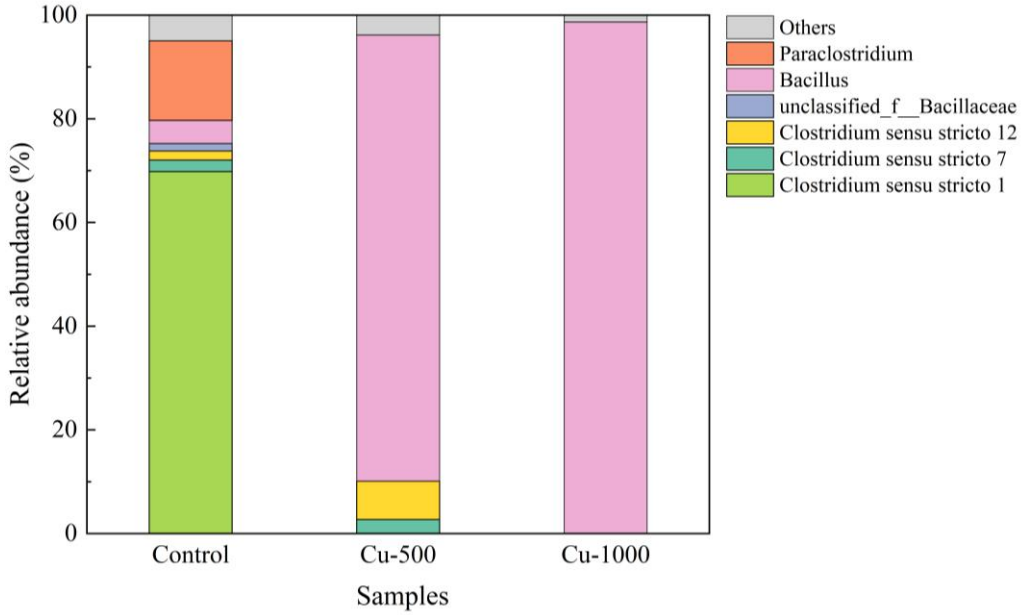
Relative abundance (%)
100
80
60
40
20
0
Control
Cu-500
Cu-1000
Samples
Others
Paraclostridium
Bacillus
unclassified_f__Bacillaceae
Clostridium sensu stricto 12
Clostridium sensu stricto 7
Clostridium sensu stricto 1

Fig. 5

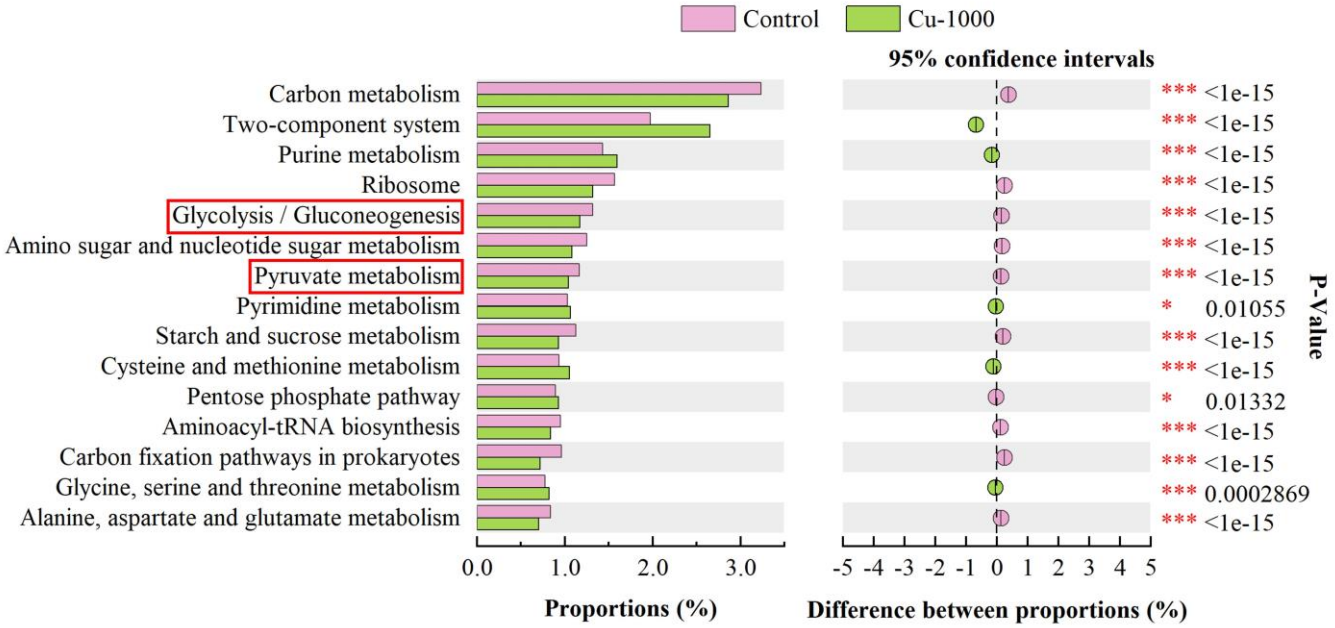
Control
Cu-1000
95% confidence intervals
Carbon metabolism
Two-component system
Purine metabolism
Ribosome
Glycolysis / Gluconeogenesis
Amino sugar and nucleotide sugar metabolism
Pyruvate metabolism
Pyrimidine metabolism
Starch and sucrose metabolism
Cysteine and methionine metabolism
Pentose phosphate pathway
Aminoacyl-tRNA biosynthesis
Carbon fixation pathways in prokaryotes
Glycine, serine and threonine metabolism
Alanine, aspartate and glutamate metabolism
*** <1e-15
*** <1e-15
*** <1e-15
*** <1e-15
*** <1e-15
*** <1e-15
*** <1e-15
* 0.01055
*** <1e-15
*** <1e-15
* 0.01332
*** <1e-15
*** <1e-15
*** 0.0002869
*** <1e-15
P-Value
0.0 1.0 2.0 3.0
Proportions (%)
-5 -4 -3 -2 -1 0 1 2 3 4 5
Difference between proportions (%)

Fig. 6

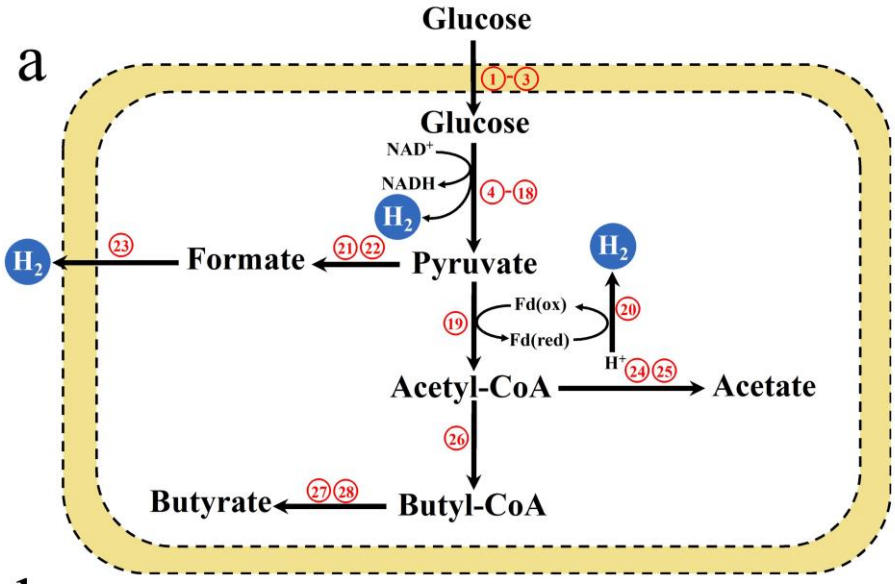

b

	Gene annotation	Gene
1	glucose/mannose transport system substrate-binding protein	K17315(gtsA)
2	glucose/mannose transport system permease protein	K17316(gtsB)
3	glucose/mannose transport system permease protein	K17317(gtsC)
4	hexokinase	K00844(HK)
5	polyphosphate glucokinase	K00886(ppgK)
6	glucose-6-phosphate isomerase, archaeal	K06859(pgi1)
7	glucose-6-phosphate isomerase	K13810(tal-pgi)
8	glucose-6-phosphate isomerase	K15916(pgi-pmi)
9	ATP-dependent phosphofructokinase	K21071(pfk)
10	ADP-dependent phosphofructokinase	K00918(pfkC)
11	fructose 1,6-bisphosphate aldolase	K01622(K01622)
12	fructose-bisphosphate aldolase, class I	K11645(fbaB)
13	glyceraldehyde-3-phosphate dehydrogenase (NAD(P)+)	K00150(gap2)
14	phosphoglycerate kinase	K00927(PGK)
15	2,3-bisphosphoglycerate-dependent phosphoglycerate mutase	K15634(gpmB)
16	2,3-bisphosphoglycerate-independent phosphoglycerate mutase	K15635(apgM)
17	enolase	K01689(ENO)
18	pyruvate kinase	K00873(PK)
19	pyruvate-ferredoxin oxidoreductase	K03737(por)
20	ferredoxin hydrogenase	K00532(E1.12.7.2)
21	formate C-acetyltransferase	K00656(E2.3.1.54)
22	pyruvate formate lyase activating enzyme	K04069(pflA)
23	formate dehydrogenase major subunit	K00123(fdoG)
24	phosphate acetyltransferase	K13788(pta)
25	acetate kinase	K00925(ackA)
26	butyryl-CoA dehydrogenase	K00248(ACADS)
27	phosphate butyryltransferase	K00634(ptb)
28	butyrate kinase	K00929(buk)